Resolving multiple sources of solar relativistic particles with implication for GLE origins

Leon Kocharov and Ilya Usoskin
Sodankylä Geophysical Observatory (Oulu Unit), University of Oulu
Oulu, Finland

Andreas Klassen
Institut für Experimentelle und Angewandte Physik, Christian-Albrechts-Universität
Kiel, Germany

Eino Valtonen
Space Research Laboratory, University of Turku
Turku, Finland

34th International Cosmic Ray Conference

30 July 2015

The Hague, The Netherlands

Instrumentation for solar high-energy particle measurements

Instrument	Advantages	Disadvantages
Neutron monitor network	Continuous observations. Angular resolution.	No abundance measurements.
SOHO/ERNE	Continuous observations. Differential measurements including direction.	Limited dynamic range.
GOES	Continuous observations. Wide dynamic range.	Wide energy channels, secondary channels.
PAMELA	Differential measurements including direction.	Low orbit.
~~AMS~~	Differential measurements including direction.	Low orbit, Data policy
SOHO/EPHIN	Wide range differential measurements.	No directional measurements.

Method

Interplanetary transport and registration modeling

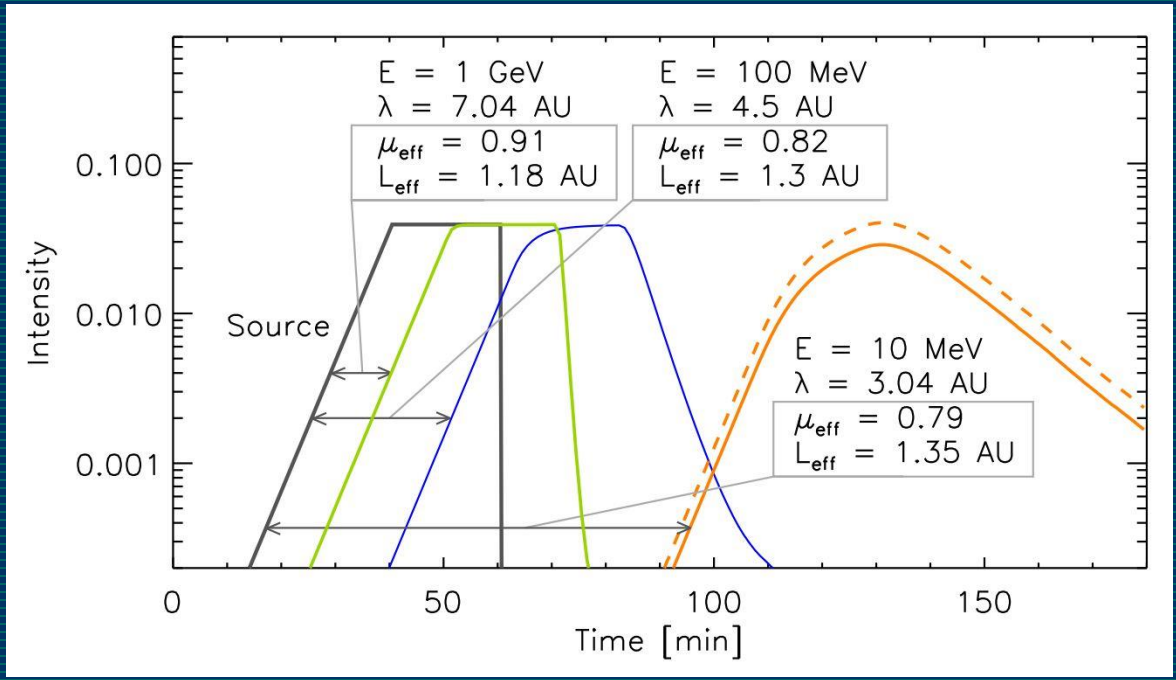

Simulated time-intensity profiles of 10 MeV, 100 MeV and 1 GeV protons arriving at the Earth's orbit from the near-Sun source. Protons are registered within the ERNE/HED view cone. Interplanetary magnetic field makes the angle of 60° with the axis of detector's view cone. Solar wind speed is 600 km/s.

$$t_s = t - \Delta t, \text{ where } \Delta t = L_{\text{eff}}/v - 8.3 \text{ min}$$

13 Dec 2006 SEP-GLE event (GLE 70)

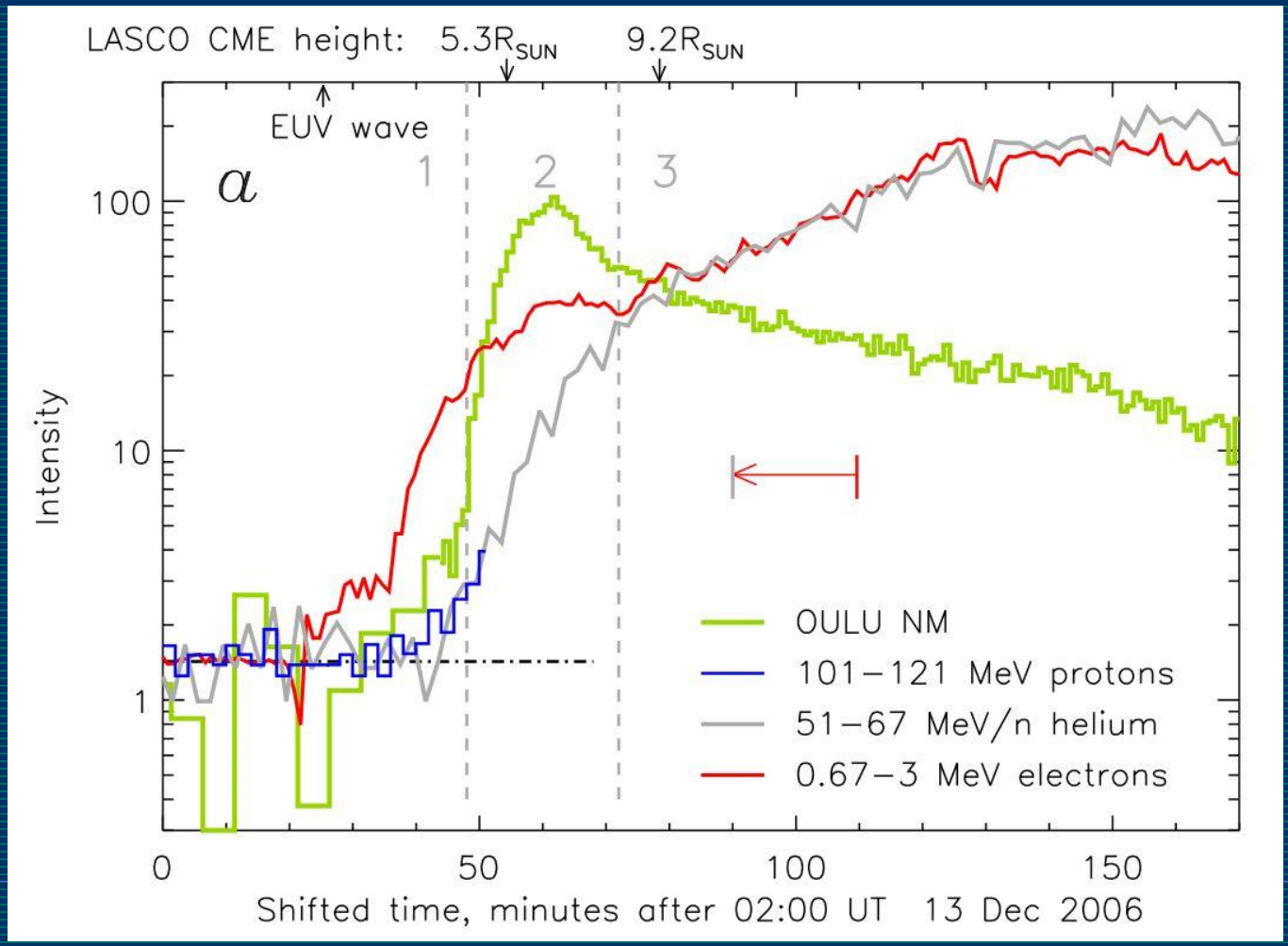

13 Dec 2006 SEP-GLE event (GLE 70)

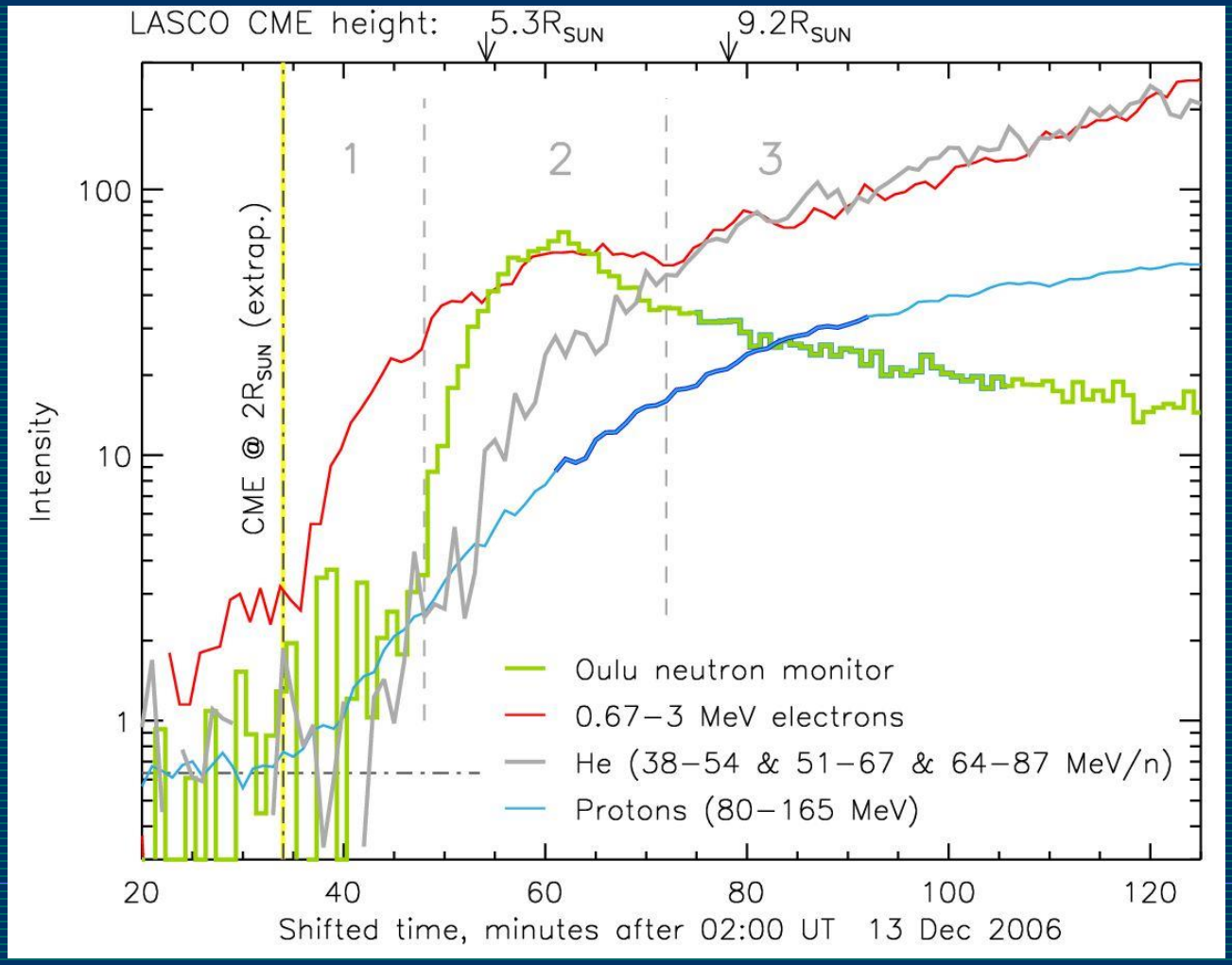

2 May 1998 SEP-GLE event (GLE 56)

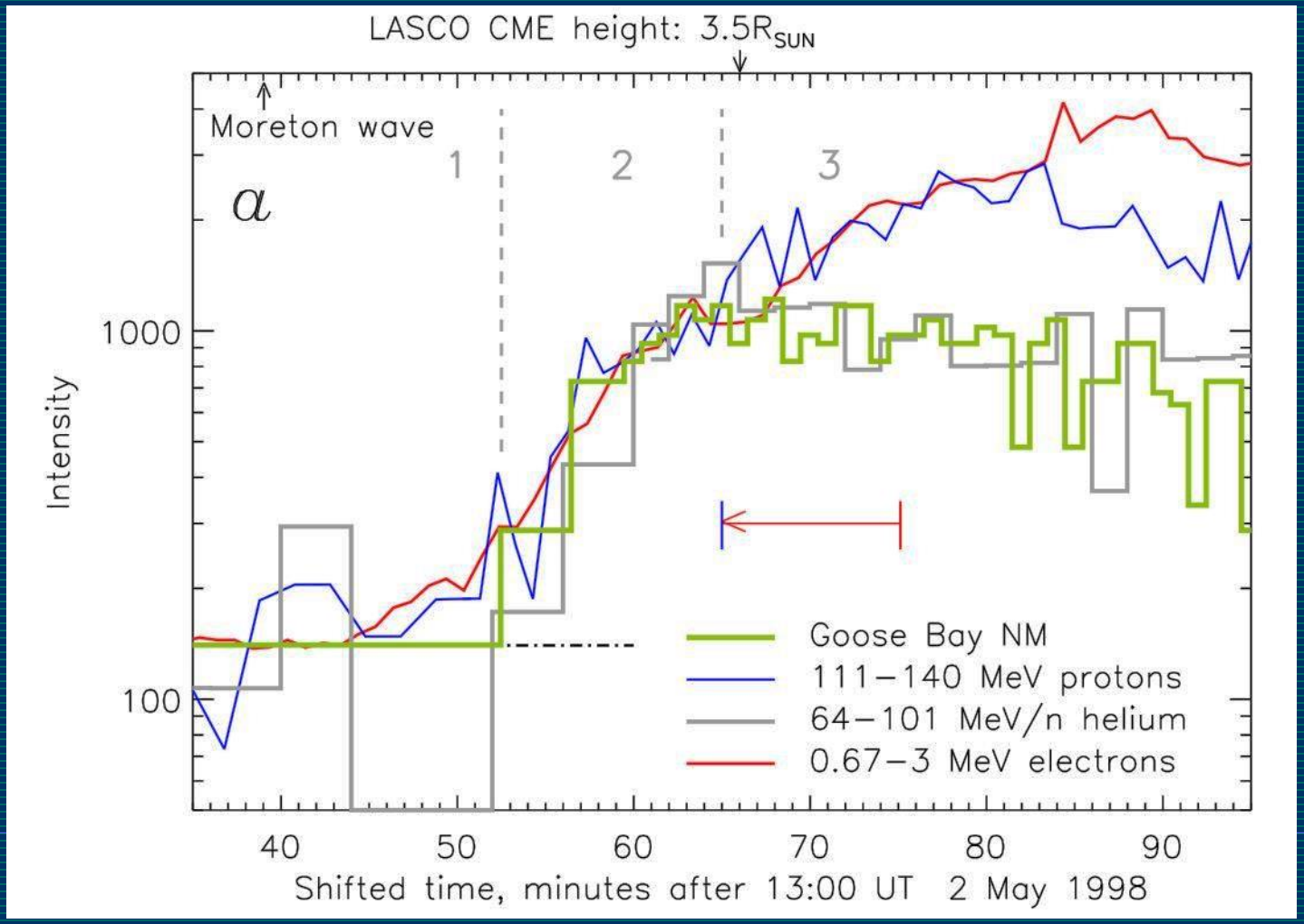

Conclusions

- Timing of ``first'' particles is not very helpful when applied to prolonged SEP emission and may be even misleading in the case of multiple injections.
- Neither direct flare particle nor particles accelerated by the CME shocks in solar wind are responsible for GLEs.
- GLEs originate from an another, third source, situated between flare and CME bow shock within a few solar radii from the Sun.
- Possible candidates are the shock interaction with a preceding structure or/and opening of a magnetic trap.

GLE 70

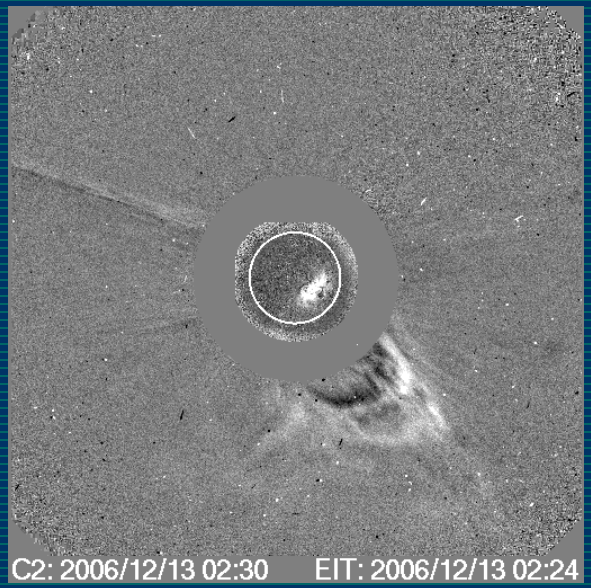
C2: 2006/12/13 02:30
EIT: 2006/12/13 02:24

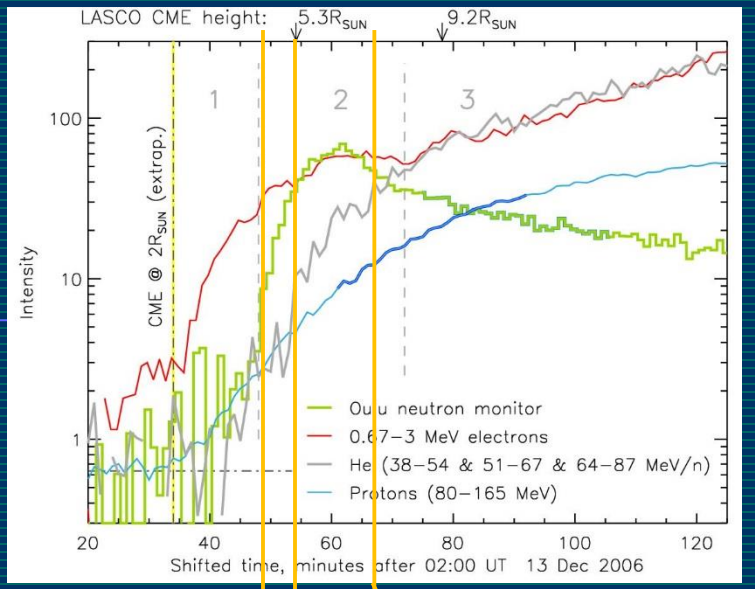
LASCO CME height:
5.3R$_{SUN}$
9.2R$_{SUN}$
1
2
3
100
10
1
Intensity
CME @ 2R$_{SUN}$ (extrap.)
Oulu neutron monitor
0.67–3 MeV electrons
He (38–54 & 51–67 & 64–87 MeV/n)
Protons (80–165 MeV)
20
40
60
80
100
120
Shifted time, minutes after 02:00 UT 13 Dec 2006

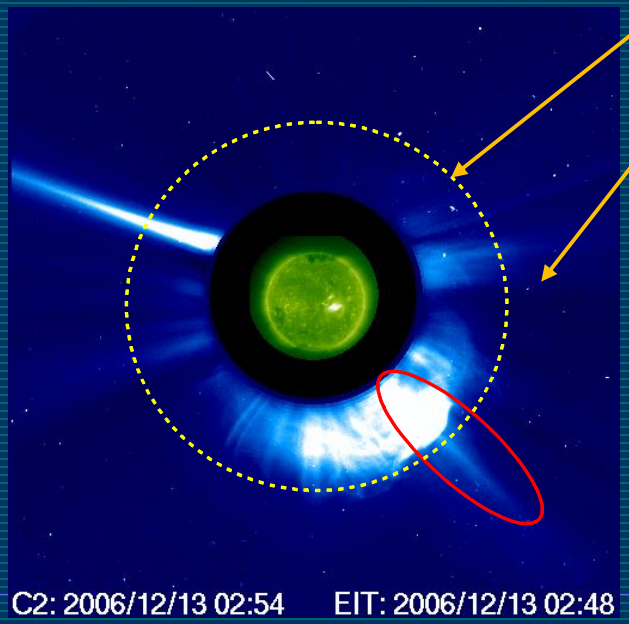
C2: 2006/12/13 02:54
EIT: 2006/12/13 02:48

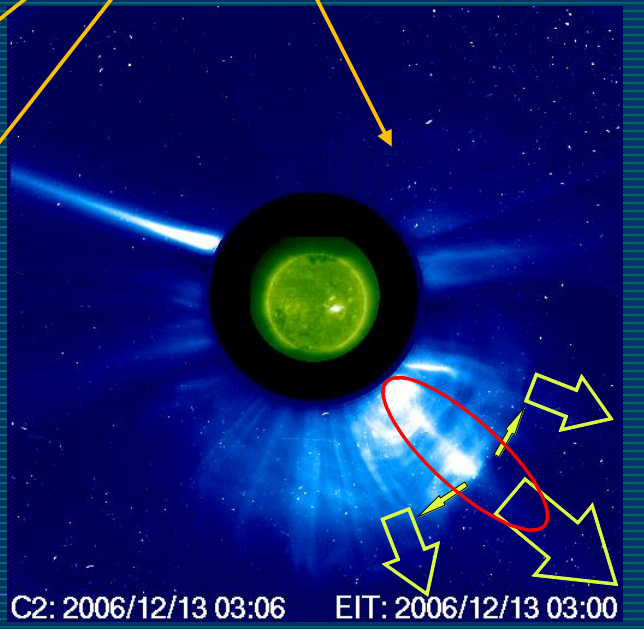
C2: 2006/12/13 03:06
EIT: 2006/12/13 03:00

The 24 May 1990 event

- Unique solar neutron event of 24 May 1990 [Shea, Smart, & Pyle (1993) GRL, 18, 1655].
- Joint analysis of the high-energy neutrons and neutron-decay protons of the 24 May 1990 event [L. Kocharov, J. Torsti, R. Vainio, G. Kovaltsov, I. Usoskin (1996) Solar Phys., 169, 181].
- The 24 May 1990 solar cosmic-ray event [J. Torsti, L. Kocharov, R. Vainio, A. Anttila, G. Kovaltsov (1996) Solar Phys., 166, 135].
- An interpretation of the 1990 May 24 event [L.Kocharov, G. Kovaltsov, J. Torsti, I. Usoskin, H. Zirin, A. Anttila, & R. Vainio (1996) in *High Energy Solar Physics*, eds. R.Ramaty, N. Mandzhavidze and X.-M. Hua, AIP Conf. Proc. 374, NY, 246-255].

The 24 May 1990 event

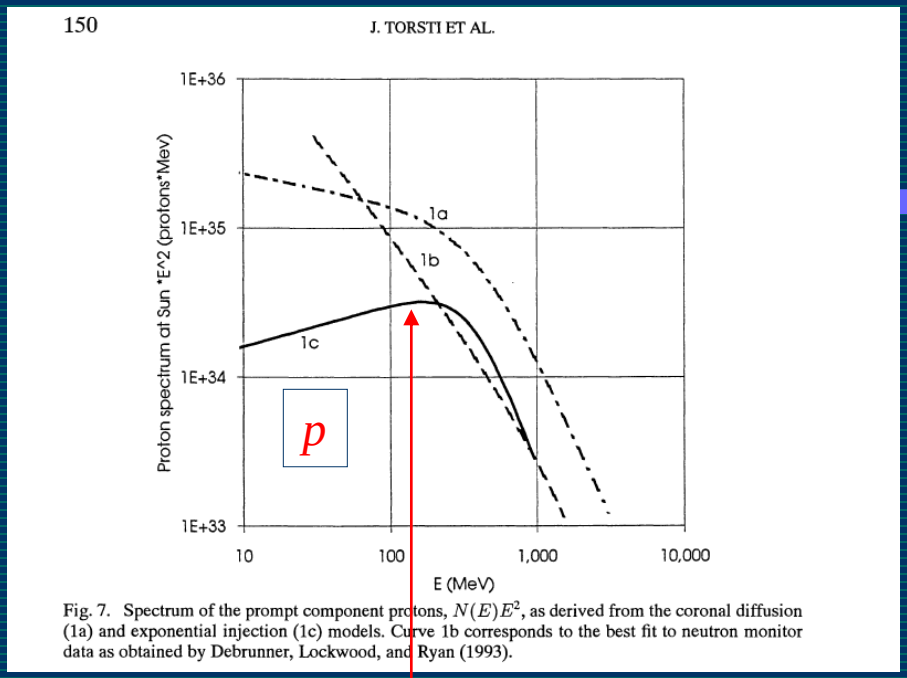

Fig. 7. Spectrum of the prompt component protons, $N(E)E^2$, as derived from the coronal diffusion (1a) and exponential injection (1c) models. Curve 1b corresponds to the best fit to neutron monitor data as obtained by Debrunner, Lockwood, and Ryan (1993).

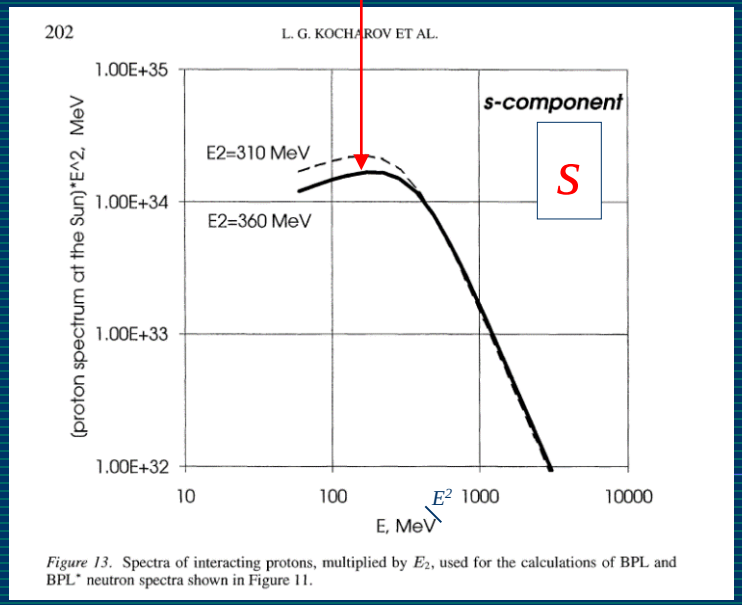

Figure 13. Spectra of interacting protons, multiplied by E_2, used for the calculations of BPL and BPL* neutron spectra shown in Figure 11.

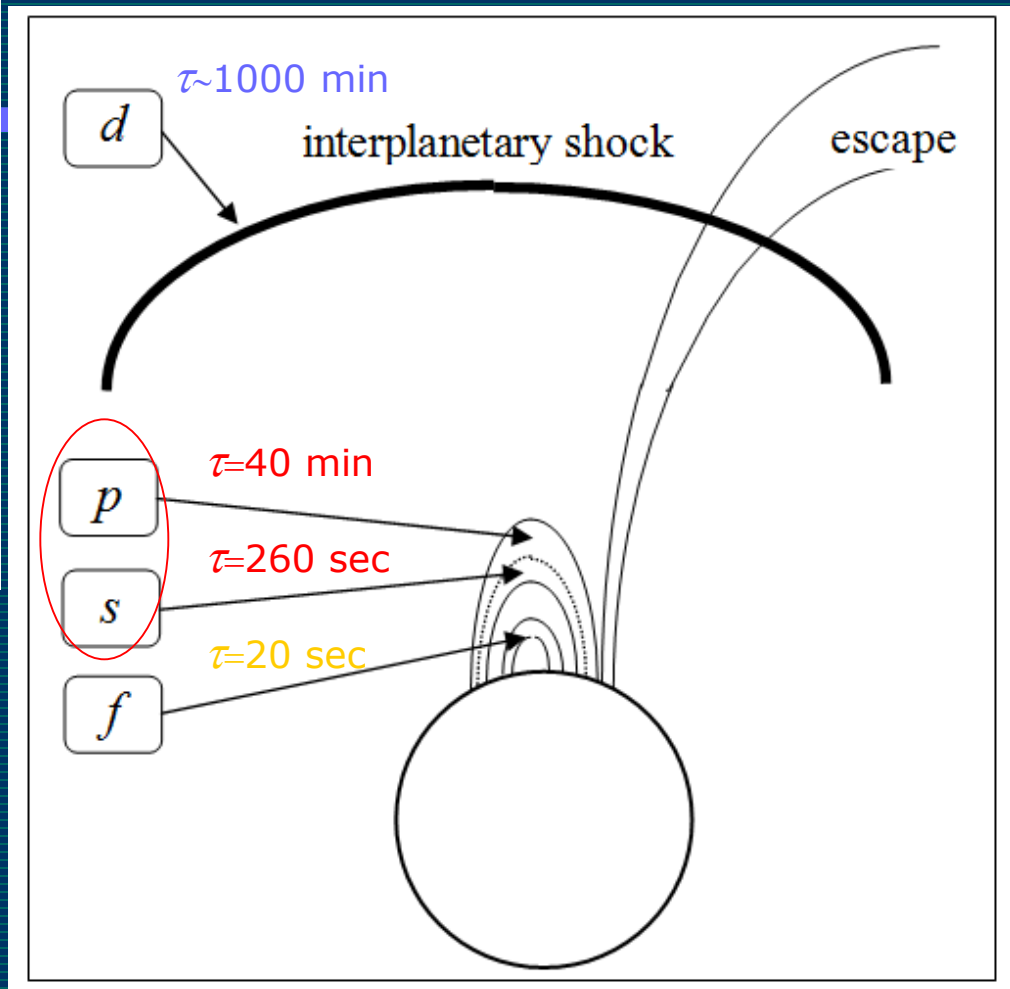

FIG. 6. Illustration of a multicomponent nature of proton production during the 1990 May 24 solar flare and cosmic ray event. Letters denote regions of acceleration or trapping of first (f-) and second (s-) components of interacting protons, prompt (p-) and delayed (d-) components of protons in the interplanetary medium.

Stochastic re-acceleration of shock-accelerated protons in magnetic loop

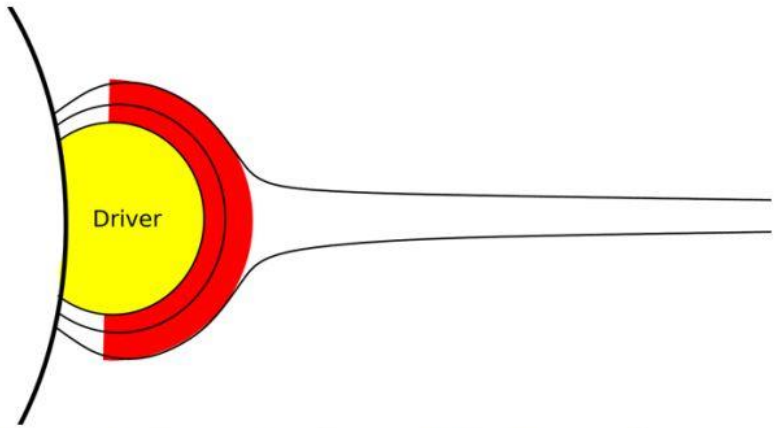

Figure 1. Formulation of the problem: a shock driven by a coronal mass ejection propagates through a coronal magnetic loop. The shock's downstream region is schematically indicated in red. Here the shock-accelerated particles are re-accelerated by the turbulence amplified by the shock.

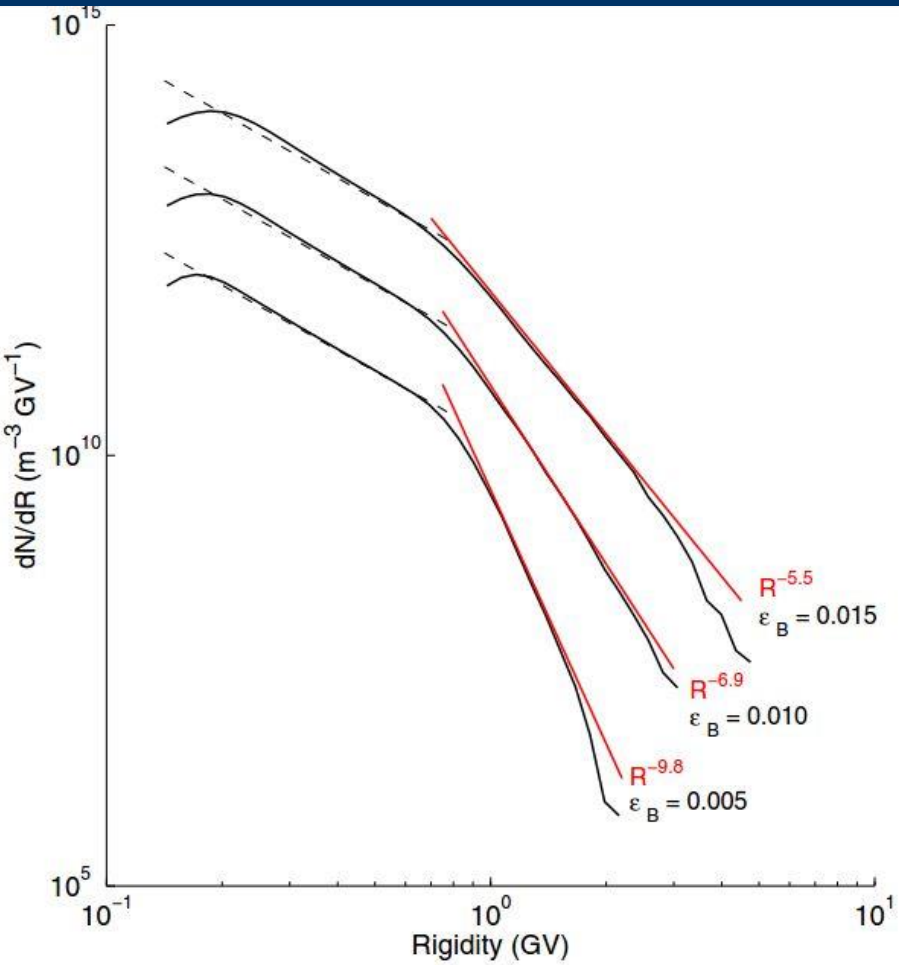

Figure 10. Resulting differential rigidity spectra of protons obtained for different values of the intensity of magnetic fluctuations ε_B: $\varepsilon_B = 0.005$ ($\alpha = 24.6$), $\varepsilon_B = 0.010$ ($\alpha = 12.3$), and $\varepsilon_B = 0.015$ ($\alpha = 8.2$). The spectrum evolution time is $\tau_{st} \approx 12$ s. The shock-accelerated proton spectrum is defined by $E_{min} = 10$ MeV, $E_{max} = 300$ MeV, $n_p = 2.1 \times 10^{11}$ m^{-3}, and $\gamma = 1.75$ in all three cases. The values of the other model parameters correspond to the primary set of values. For better visualization, the spectra in the cases of $\varepsilon_B = 0.010$ and $\varepsilon_B = 0.015$ are shifted along the ordinate axis by being multiplied by the coefficients of 10 and 100, respectively. The spectra are fitted at high rigidities by power-law functions shown in red.

A. Afanasiev, R. Vainio, and L. Kocharov (2014) ApJ, 790, 36

CORE PLUS HALO MODEL OF DIFFUSIVE SHOCK ACCELERATION AND STOCHASTIC RE-ACCELERATION

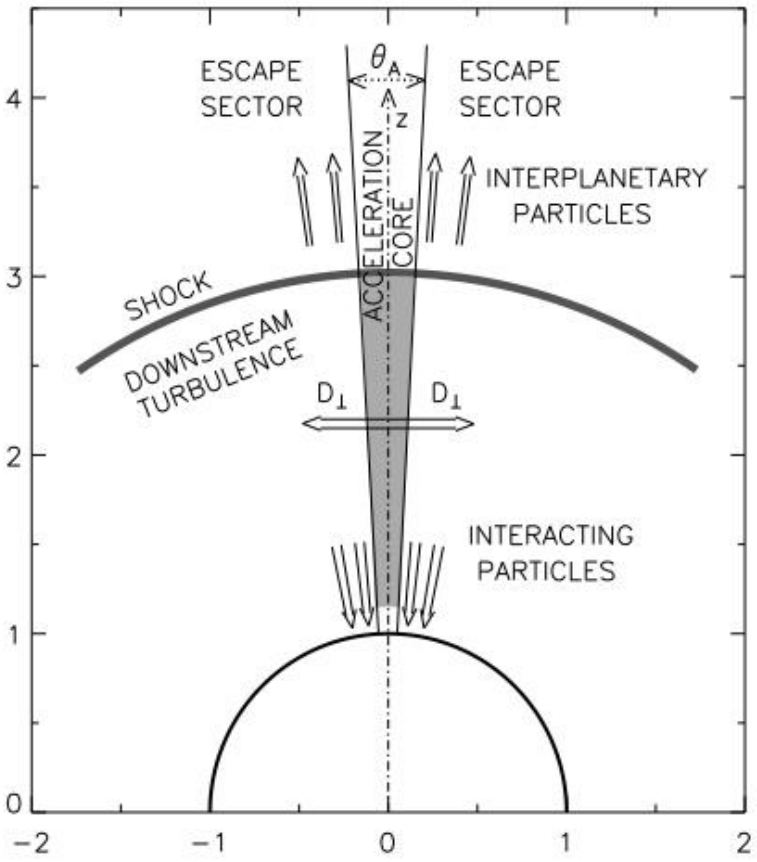

Fig. 1.— Particle acceleration and transport model. Shaded is the region of stochastic re-acceleration of the shock accelerated particles. Effective depth of this region is consistent with the proton energy spectrum and hence depends on the energy of resonant protons.

$D_{HALO}/D_{CORE}=50$,
$D_{1,CORE}(0.1\ MeV)=2*10^6\ km^2/s$

L. Kocharov, T. Laitinen, A. Afanasiev, R. Vainio, K. Mursula, and J.M. Ryan (2015) ApJ, 806, 80